Desalination and Water Treatment
www.deswater.com
doi: 10.5004/dwt.2023.29547

295 (2023) 83–94
May

Numerical simulation and experimental optimization of ultrasonic cracking in excess sludge

Nan Zhang[a,b], Ying Qin[c], Yun Wan[a,b], Wei Wei[a,b], Shuguang Zhu[a,b,c,*], Kefeng Lu[b,d], Zhiwei Wang[b]

[a]*Anhui Key Laboratory of Water Pollution Control and Wastewater Recycling, Anhui Jianzhu University, Hefei, Anhui 230601, China, Tel.: +00-86-0551-63513118; emails: zhushuguang@ahjzu.edu.cn/286537056@qq.com (S. Zhu), 1529253431@qq.com (N. Zhang)*
[b]*School of Environment and Energy Engineering, Anhui Jianzhu University, Hefei, Anhui 230601, China, Tel.: +00-86-0551-63828123*
[c]*School of Mechanical and Electrical Engineering, Anhui Jianzhu University, Hefei, Anhui 230601, China, Tel.: +00-86-0551-63828083*
[d]*Anhui Institute of Strategic Study on Carbon Dioxide Emissions Peak and Carbon Neutrality in Urban-Rural Development, Anhui Jianzhu University, Hefei, Anhui 230601, China, email: rongnai@ahjzu.edu.cn*

Received 9 October 2022; Accepted 7 April 2023

ABSTRACT

Ultrasonic treatment of municipal sludge can effectively reduce the moisture content, improve sludge stability, and create optimal conditions for subsequent sludge disposal. Methods to optimize the ultrasonic treatment of excess sludge have great practical significance. This study determined the influence of ultrasonic frequency, the axial distance between the thermal and ultrasonic probes, ultrasonic power, and other factors involved in cavitation experiments, The MATLAB and FLUENT software were used to simulate the ultrasonic sludge treatment effects under varying conditions; these simulations were verified by microscopic and biochemical analyses. The results showed that lower frequency and higher power yielded stronger temporal and spatial effects; the optimal conditions were 20 kHz and 1,000 W. After 30 min of treatment, the sludge particle size was significantly reduced, with d_{50} decreasing from 34.82 μm in the original sludge to 2.99 μm, and a small number of nanoscale particles formed. Therefore, ultrasonic treatment yields an excellent cracking effect on excess sludge. The results of simulation analysis and experiments can provide a reference to achieve effective stabilization, resource utilization, safety, and excess sludge reduction.

Keywords: Ultrasonic cracking; Excess sludge; Numerical simulation; Cavitation effect

1. Introduction

Although the continuous advancement in sewage treatment procedures has improved the sewage collection and treatment rate, the subsequent generation of excess sludge poses a huge problem [1]. Excess sludge contains many harmful substances, such as chemical and biological waste, toxic elements, and pathogenic microbes; hence, appropriate sludge treatment and disposal procedures are essential for improving urban development [2]. Sludge should be treated appropriately to achieve the goal of sludge disposal based on subsequent stabilization, resource utilization, harmlessness, and sludge reduction [3].

Cracking excess sludge is an effective pretreatment process in sludge recycling and reduction. In recent years, ultrasonic pretreatment of residual sludge has received a

* Corresponding author.

1944-3994/1944-3986 © 2023 Desalination Publications. All rights reserved.

great deal of attention due to its low environmental impact, high energy density, mild reaction conditions, and high efficiency [4]. An ultrasonic wave is a sound wave ranging from 20 kHz to 10 MHz. When it acts on excess sludge, it can destroy the cell structure of microorganisms, change their activity, and release intracellular substances. Several studies have shown that the cracking effect of ultrasonics on the sludge is mainly based on the ultrasonic cavitation effect. That is, when a certain intensity of ultrasonic wave acts on excess sludge, a large number of cavitation bubbles are generated inside, which vibrate continuously under the action of ultrasonic wave. When the sound pressure exceeds the threshold, it is violently compressed, expanded, and then instantly cracked [5]. The cavitation effect produces strong shock waves and arrives at the local high temperature and high pressure that can destroy the cellular structure of microorganisms and inactivate pathogenic bacteria [6]. At present, many studies reported on ultrasonic sludge cracking techniques. Skórkowski et al. [7] evaluated the relationship between ultrasonic cracking effects and other energy parameters. Bhat and Gogate [8] studied the effect of cavitation effects on biological processes, and Yuan et al. [9] analyzed the effect of ultrasonic treatment combined with hydrogen peroxide on excess sludge fragmentation. However, there are still some weaknesses in the distribution and form of action of ultrasonic energy; therefore, there is an urgent need to explore the distribution patterns of ultrasonic treatment and the visualization of cavitation bubbles to optimize the conditions for ultrasonic cavitation effects, which may provide new solutions for wastewater treatment.

Based on MATLAB and FLUENT software, which were used to simulate the ultrasonic cavitation conditions for visualization and analysis, this study investigated and analyzed the ultrasonic frequency, ultrasonic power, and other factors to optimize the process of ultrasonic cracking of excess sludge and analyzed the morphology and particle size of the sludge before and after ultrasonic cracking. In addition, we aimed to build our own experimental device to explore the variation law of cavitation effect intensity along the axial direction under different conditions. We validated and characterized the ultrasonic cavitation effect through experiments, providing substantial evidence and technical protocols that will support future research regarding ultrasonic cracking for sludge disposal.

2. Material and methods

2.1. Material

Excess sludge was taken from the secondary sedimentation tank of a Hefei Sewage Treatment Plant as the experimental sample. The main characteristic indexes were recorded as temperature: 15°C; pH: 7.10; moisture content: 97%; density: 1.035×10^3 kg/m^3; dissolved chemical oxygen demand (SCOD): 96 mg/L.

2.2. Generation of cavitation effect

The cavitation effect is the main mechanism underlying ultrasonic sludge cracking, and the process of its generation is shown in Fig. 1. Ultrasonic refers to a longitudinal wave that propagates in the liquid phase; the propagation direction does form two phases of compression and expansion, so that the liquid is in two states with positive and negative pressure, respectively. When the ultrasonic waves are in the negative expansion phase, the ultrasonic pressure amplitude exceeds the internal static pressure of the liquid, and the distance between the molecules of the liquid in the expansion phase vibration is greater than the spacing that allows the liquid to maintain a positive pressure state, resulting in the integrity of the liquid structure being destroyed, forming new small cavitation nuclei. In the ultrasonic expansion state, these cavitation nuclei and the original microbubbles in the liquid expand rapidly, whereas then the volume rapidly collapses in the compression state, resulting in local high temperature, high pressure, and shock waves, as well as the release of a large amount of energy to form new cavitation nuclei [10].

2.3. Characterization of cavitation effects

The basic condition for the cavitation effect of excess sludge by ultrasonic treatment is to have sufficient sound intensity; the higher the sound intensity, the stronger the

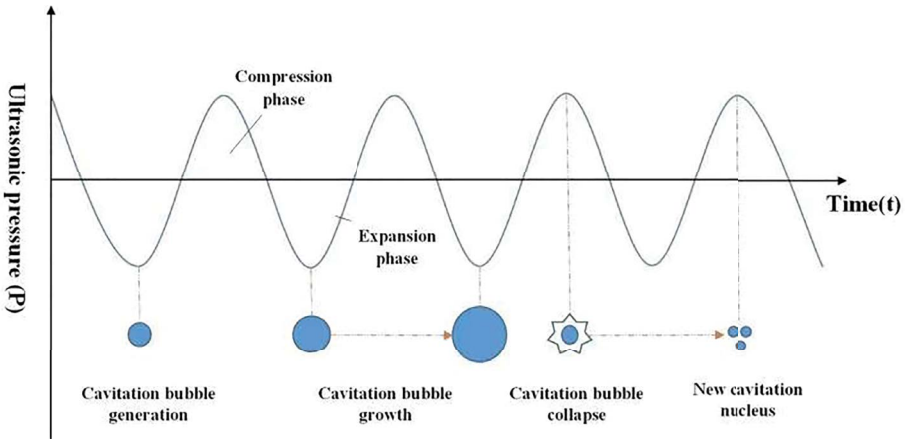

Fig. 1. Ultrasonic cavitation effect generation process.

cavitation effect. Consequently, the strength of the ultrasonic cavitation effect is often characterized by the measurement of sound intensity. The thermal probe method has the characteristics of low cost and high accuracy, and is not affected by radiation or electromagnetic fields; thus, this method is used to characterize the cavitation effect of ultrasonic treatment.

The principle underlying the thermal probe method is to establish a relationship between ultrasonic intensity and temperature based on the law of energy conservation, and to characterize the intensity of the sound field indirectly through temperature changes [11]. It consists of an electrical pair wrapped in a wave-absorbing material that absorbs the ultrasonic waves and converts the energy into thermal energy, which, in turn, is used to measure the equilibrium temperature difference through a temperature collector. The cavitation intensity at any point under different conditions can be known from the variation of the equilibrium temperature difference.

2.4. Experimental device

The experimental self-designed cavitation intensity measurement device is shown in Fig. 2. The setup mainly comprises an ultrasonic device, a thermocouple coated with absorbing material, and a temperature collector. The ultrasonic probe is placed in the center of the cylindrical beaker, and the thermocouple wrapped with absorbing material is placed directly below the ultrasonic probe. The thermocouple can convert sound waves into temperature, which can be converted into electrical signals. By measuring the electrical signals, we can know the intensity of the cavitation effect. The ultrasonic generator is a probe-type ultrasonic reactor (model: DH99-IIDN) with a power adjustment range of 0–1,200 W. The reaction vessel is a 500 mL cylindrical glass beaker. Ultrasonic probes of 20 and 24 kHz were used in the experiment, and 400 mL sludge was put into a reaction vessel without temperature control.

The self-designed ultrasonic experimental setup is shown in Fig. 3, in which the ultrasonic generation device is the same as above, an ultrasonic variable amplitude rod with a frequency of 20 kHz and a probe diameter of 22 mm is used, and the reaction vessel is a 500 mL cylindrical glass beaker.

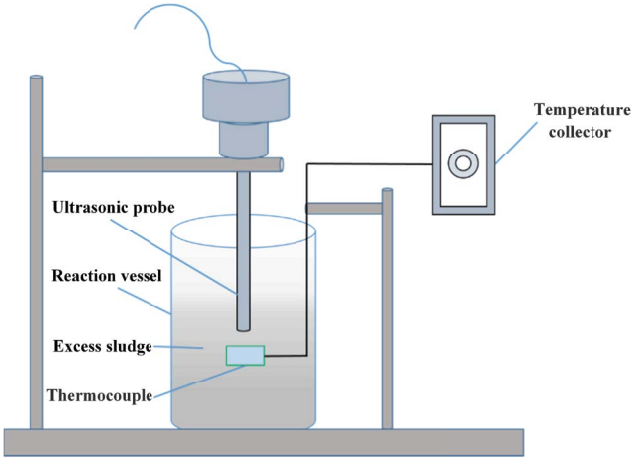

Fig. 2. Diagram of ultrasonic cavitation experimental device.

2.5. Ultrasonic cavitation bubble kinetic model

The purpose of studying bubble dynamics is to investigate the motion of bubbles under the action of ultrasonic treatment through the equation of motion of bubble walls, and the intensity of motion of cavitation bubbles represents the ultrasonic cavitation intensity.

The bubble dynamic was first modeled by the British Physicist Rayleigh in 1917, and then the scientist Plesset made a series of corrections based on this equation to arrive at the famous Rayleigh–Plesset equation [12]; the equation is as follows:

$$\frac{P_B(t)-P_\infty(t)}{\rho_L}=R\frac{d^2R}{dt^2}+\frac{3}{2}\left(\frac{dR}{dt}\right)^2+\frac{4\nu_L}{R}\frac{dR}{dt}+\frac{2S}{\rho_L R}$$

where $P_B(t)$ is the pressure inside the microbubble; $P_\infty(t)$ is the pressure outside the microbubble; ρ_L is the density of the medium around the microbubble; $R(t)$ is the microbubble radius; ν_L is the medium viscosity; S is the tension on the surface of the microbubble.

This equation assumes that the medium is a Newtonian fluid, homogeneous and incompressible, and that there is no tissue around the microbubble and other microbubbles influence; for a single microbubble, it is assumed that the microbubble is spherical and that there is only radial vibration when vibrating with $R(t)$.

In recent years, most numerical simulations of cavitation bubbles have been based on the Rayleigh–Plesset equation using the simulation software MATLAB for numerical solutions. For example, based on this equation, Yi et al. [13]

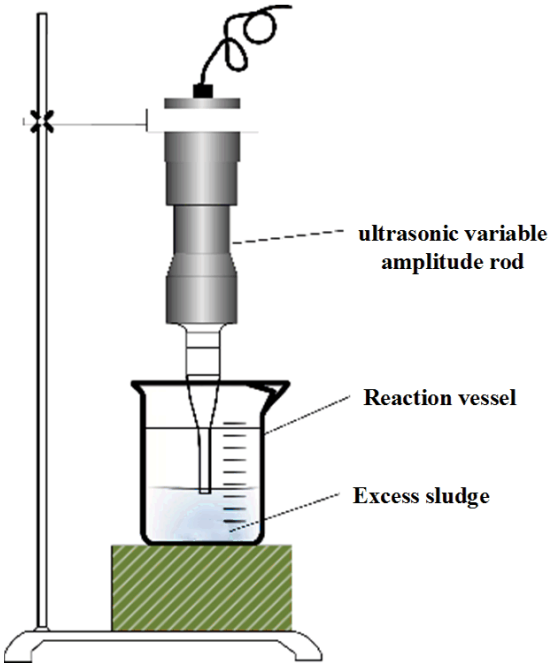

Fig. 3. Ultrasonic experimental set-up diagram.

analyzed the effect of liquid viscosity on the strength of ultrasonic cavitation using MATLAB software. They concluded that the medium could enhance the cavitation and fragmentation effects under ultrasonic action; however, it also affects the ultrasonic wave conduction, causing the cavitation effect to decrease.

2.6. MATLAB software simulation

MATLAB software was used to simulate different ultrasonic frequencies and power, and the effect on the ultrasonic cavitation effect was analyzed by examining the cavitation bubble transient radius and the amplitude of cavitation bubble motion. The ultrasonic frequencies used in the simulation model were 20, 24, 28, and 30 kHz, with ultrasonic power usage at 400, 600, 800, and 1,000 W, respectively. The 4–5 order Runge–Kutta algorithm was used to solve the nonlinear motion cavitation bubble equations, and MATLAB calculation algorithms and function programs were designed [14,15].

2.7. FLUENT software simulation

With the mature development of computational fluid dynamics, FLUENT software has gradually been used in the numerical simulation of cavitation bubbles, which is suitable for simulating complex fluid flows with its powerful mesh support and multiple algorithms. Therefore, FLUENT software was used to simulate the morphological changes of cavitation bubbles in one cycle. The effects of different ultrasonic power and frequency on the morphological changes of cavitation bubbles were also analyzed.

The ICEM preprocessor in FLUENT software was used to establish the model, with set boundaries and a divided grid. The established model is shown in Fig. 4a. The model is set as a square region with a side length of L = 0.4 mm, and a spherical cavitation bubble with an initial radius of R = 20 μm. The boundary conditions are set as follows: JK is the pressure inlet, EF is the pressure outlet, and EJ and FK are non-slip walls. A two-dimensional structured grid is used to discretize the geometric structure. The grid size is 6.4 × 10^{-13} m^2, and the total number of grids is 2.5 × 10^5. The divided grid diagram is shown in Fig. 4b.

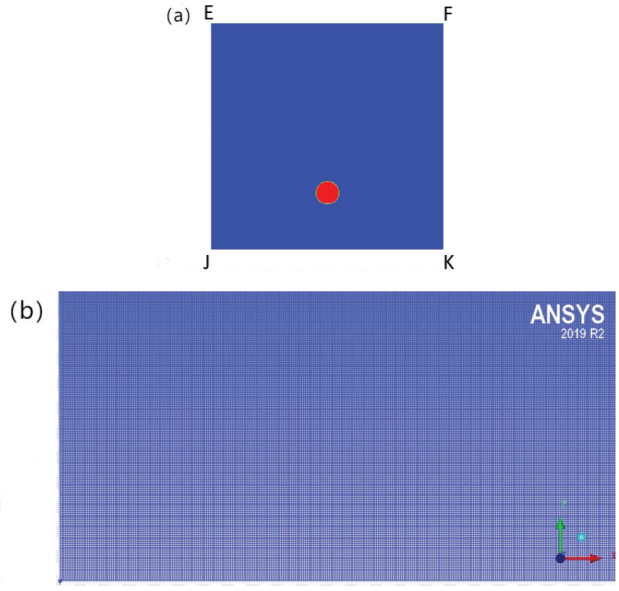

Fig. 4. Fluent models of (a) geometric model and (b) grid division diagram.

In order to solve the change of the interface between the gas and liquid phases of the cavitation bubble, it is assumed that the interface of the cavitation bubble is a free surface, and the initial state of the cavitation bubble is in an expanded state, ignoring the action and influence of various forces. VOF two-phase model is adopted in the calculation model, in which the gas phase is an ideal gas as the main phase and the incompressible liquid Newtonian fluid as the auxiliary phase [16]. The turbulence model adopts the standard k–ε model. The pressure value is estimated using PRESTO! algorithm. PRESTO! is an implicit operator segmentation algorithm that provides values for velocity and pressure combinations [17]. In the calculation, the first-order implicit and second-order upwind schemes were adopted in time and space, respectively.

2.8. Ultrasonic crack experimental methods

- Placed 400 mL of sludge in a 500 mL glass beaker, the probe-type ultrasonic generator was fixed, and lower the ultrasonic probe down to 2 cm below the liquid.
- The ultrasonic generator was turned on at room temperature, the ultrasonic time was set from 0 to 30 min, and the ultrasonic power was set from 270 to 900 W, using a 20 kHz, 22 mm diameter variable amplitude rod for ultrasonic treatment of the experimental sludge.
- After the ultrasonic treatment, the ultrasonic probe was removed, the treated sludge was collected and centrifuged, and the supernatant, after centrifugation, was stored for testing. The purity of the reagents used in the experimental process was of analytical grade.

3. Results and discussion

This section demonstrates the cycle variation of cavitation bubbles at various ultrasonic frequencies and ultrasonic powers, followed by cavitation experimental results that were used to validate the simulation effect. Finally, the sludge cracking effect was depicted from microscopic and biochemical perspectives.

3.1. MATLAB simulation analysis

The ratio of instantaneous radius to the initial radius of a cavitation bubble, that is, the amplitude of cavitation bubble motion, was used to characterize the cavitation effect of the cavitation bubble. Taking time as the abscissa and cavitation bubble amplitude as the ordinate, the motion of the ultrasonic cavitation bubble was simulated by changing ultrasonic power and frequency.

3.1.1. Effect of ultrasonic frequency

The ultrasonic power was regulated at 1,000 W, and the ultrasonic frequency (20, 24, 28, and 30 kHz) was changed

to study their influence on the ultrasonic cavitation effect. The simulation results are shown in Fig. 5.

As seen in Fig. 5, when other factors are kept constant, the amplitude of the cavitation bubble changes consistently under four ultrasonic frequencies. With the increase of ultrasonic frequency, the amplitude of the cavitation bubble decreases, the time to reach the maximum amplitude becomes longer, the cracking time becomes longer, and the ultrasonic cavitation effect becomes weaker. The main reason is that the expansion time of the ultrasonic phase becomes shorter with the increase of ultrasonic frequency, and the high-frequency ultrasonic wave decays rapidly when propagating in the liquid medium, thus weakening the ultrasonic cavitation effect [18]. Therefore, when other conditions are constant, using a lower-frequency ultrasonic wave would yield a better ultrasonic cavitation effect. Xuefeng [19] also found that the lower the ultrasonic frequency, the earlier the cavitation bubble collapses and the smaller the cavitation bubble amplitude, and that the lowest possible frequency can maximize the ultrasonic effect while meeting cavitation requirements. In this simulation, when the ultrasonic frequency is 20 kHz, the collapse period of the cavitation bubble is the shortest, and the motion amplitude of the cavitation bubble is the largest; hence, the best ultrasonic cavitation effect is achieved.

3.1.2. Effect of ultrasonic power

The influence of ultrasonic power (400, 600, 800 and 1,000 W) on ultrasonic cavitation was studied by controlling the ultrasonic frequency at 20 kHz. The simulation results are shown in Fig. 5.

As seen in Fig. 5, when other factors are kept constant, the cavitation bubbles reach the maximum amplitude in the first cycle under four ultrasonic power conditions. With the increase in ultrasonic power, the motion amplitude of cavitation bubbles becomes larger, and the ultrasonic cavitation effect becomes stronger. The main reason is that when the ultrasonic power increases, the tensile and compressive effects of cavitation bubbles in the positive and negative pressure areas of ultrasonic become stronger, and the motion period becomes longer [20]. The simulation results show that when the ultrasonic power is 1,000 W under the experimental simulation conditions, the radius ratio of cavitation bubbles is the largest, the cavitation motion is more intense, and the ultrasonic effect is the best.

3.2. Fluent simulation analysis

Based on the MATLAB software simulation above, a better ultrasonic cavitation effect can be obtained under certain conditions using a lower ultrasonic frequency or larger ultrasonic power. This part aims to further simulate and discuss the best effect of cavitation bubble change under optimized conditions by FLUENT software.

3.2.1. Effect of ultrasonic power

In this simulation, the ultrasonic frequency is 20 kHz, and the influence of ultrasonic power (400 and 1,000 W) on cavitation bubble morphology is studied. The simulation results are shown in Fig. 6.

As can be seen from the two figures, the cavitation bubble remains spherical in the expansion stage and begins to sag in the contraction stage; the position of the cavitation bubble changes relative to the initial position. This is because, during the process of cavitation bubble contraction, its contraction pressure needs to overcome the expansion pressure; to achieve this, the kinetic energy of the cavitation bubble will increase, and its position will also change [21].

The cavitation bubble will not remain spherical all the time during the shrinkage process. Therefore, the deformation of the cavitation bubble can be studied by the ratio of the maximum area to the minimum area of the two-dimensional cavitation bubble section during one period to analyze the intensity of the cavitation reaction [22]. The area and ratio of cavitation bubbles under different power intensities are shown in Table 1.

From the simulation, it can be seen that the increase of ultrasonic power increases the ratio between the maximum and minimum area. Therefore, when the ultrasonic frequency is 20 kHz, the best value of the cavitation effect is achieved when the ultrasonic power is 1,000 W.

3.2.2. Effect of ultrasonic frequency

In this simulation, the ultrasonic power is 1,000 W, and the influence of ultrasonic frequency (20 and 24 kHz) on cavitation bubble morphology is studied. The simulation results are shown in Fig. 6. When the ultrasonic power is 1,000 W, the cavitation bubble area and its ratio under different ultrasonic frequencies are shown in Table 1.

From the simulation, it can be seen that the increase in ultrasonic frequency caused an evident decrease in the ratio between the maximum and minimum area. This is due to the fact that at higher frequencies, the expanding phase of the cavitation bubble becomes shorter, and the energy accumulated becomes lower, yielding a smaller maximum area. Therefore, when the ultrasonic power is 1,000 W, and the ultrasonic frequency is 20 kHz, the cavitation effect is better achieved at this lower frequency than at 24 kHz.

The simulation results of cavitation bubble motion by MATLAB and FLUENT software suggest that using low frequency (20 kHz) and high ultrasonic power (1,000 W) can enhance the ultrasonic cavitation effect.

3.3. Cavitation experimental analysis

The influence of ultrasonic frequency, ultrasonic power, and the distance between the thermocouple and ultrasonic probe on the cavitation effect was explored using the self-built ultrasonic cavitation intensity measuring device. Moreover, the ultrasonic cavitation experimental results were compared with the numerical simulation results to verify the accuracy of the simulation.

3.3.1. Change of ultrasonic frequency

Using ultrasonic power of 400, 600, 800, and 1,000 W, the ultrasonic action time is 5 s, and the ultrasonic probe insert depth is 2 cm. By changing the ultrasonic frequency (20 and 24 kHz), the variation law of the cavitation effect along the axial direction was investigated, and its influence on the

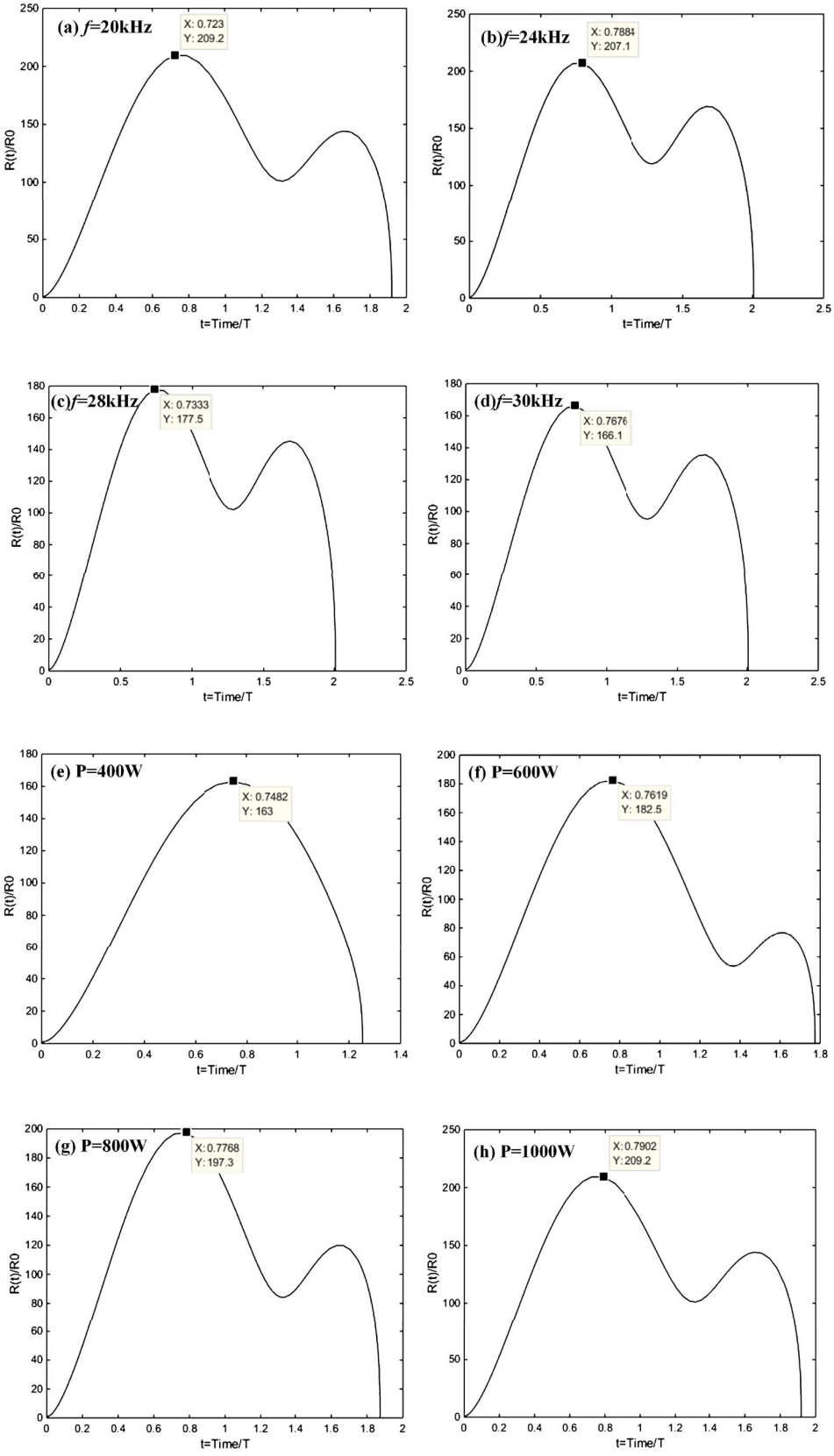

Fig. 5. Variation of cavitation bubble radius ratio with time at (a–d) different ultrasonic frequencies and (e–h) different ultrasonic power intensities.

ultrasonic cavitation effect was studied. The experimental results are shown in Fig. 7. Where the horizontal coordinate is the longitudinal distance of the thermocouple from the emitting surface, and the vertical ordinate is the equilibrium temperature difference (unit °C), which can represent the cavitation effect at each point.

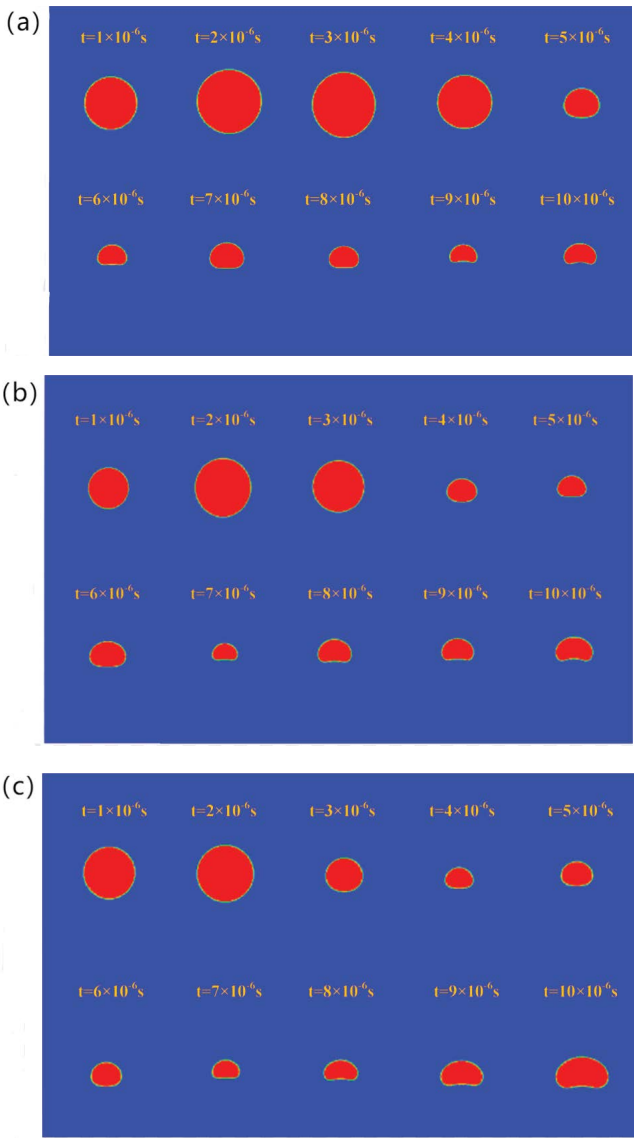

Fig. 6. The processes of cavitation bubble change at (a) f = 20 kHz, P = 400 W, (b) f = 20 kHz, P = 1,000 W and (c) f = 24 kHz, P = 1,000 W.

As seen in Fig. 7, under constant ultrasonic power, the curves of different frequencies show the same trend; the temperature difference at 20 kHz is greater than at 24 kHz, and thus the cavitation effect is stronger at 20 kHz. This shows that the ultrasonic frequency has a significant influence on the cavitation effect (the lower the frequency, the less the number of ultrasonic vibrations). This is because, at lower frequencies, a single wave must carry more energy, leading to the phenomenon of high sound intensity at lower frequencies [23]. By plotting the two-dimensional distribution of the cavitation field at different ultrasonic frequencies, Guo et al. [24] found that as the ultrasonic frequency increases, the area of the efficient ultrasonic zone gradually decreases, and the directivity of the ultrasonic worsens. Hence, the increase in ultrasonic frequency is not conducive to the cavitation effect, which is the same as the conclusion of this paper. Therefore, choosing a lower ultrasonic frequency can yield a better ultrasonic cavitation effect when other parameters are constant.

3.3.2. Changes in the distance between the thermocouple and ultrasonic probe

With other parameters kept constant, the optimized ultrasonic frequency is 20 kHz, and the ultrasonic power intensities of 400, 600, 800, and 1,000 W are adopted. The influence of the axial distance between the thermal probe and the ultrasonic probe on the ultrasonic cavitation effect is studied by changing the axial distance between the thermal and the ultrasonic probes. The experimental results are shown in Fig. 8.

As seen in Fig. 8, under different ultrasonic powers, the overall changing trend of images remains constant; the sound intensity was the largest near the ultrasonic probe but subsequently decreased with the increase in axial distance, gradually approaching a certain value at 1 cm away from the ultrasonic probe. This is because when ultrasonic waves are transmitted in excess sludge, a severe cavitation reaction occurs near the ultrasonic probe, which consumes most of the ultrasonic energy and attenuates ultrasonic energy via viscous and heat conduction absorption. In this experiment, at a 1 cm distance from the ultrasonic probe, the fluctuation of sound intensity in some areas was observed. Since the experiment was carried out in a glass beaker with limited volume, the bottom wall of the beaker and the boundary between the gas and liquid phases reflect the ultrasonic wave, resulting in sound interference [25]. The same conclusion was reached by Dong et al. [26]. They found that the general trend of sound intensity decreases with increasing axial distance at different power levels, while the smaller value added in sound intensity at about 1/2 of the ultrasonic

Table 1
Variation of cavitation bubble area under different ultrasonic conditions

Ultrasonic frequency (kHz)	Ultrasonic power (W)	Maximum area (cm²)	Minimum area (cm²)	Maximum area/Minimum area
20	400	0.02546	0.00418	6.09
20	1,000	0.01987	0.00269	7.39
24	1,000	0.01552	0.00246	6.31

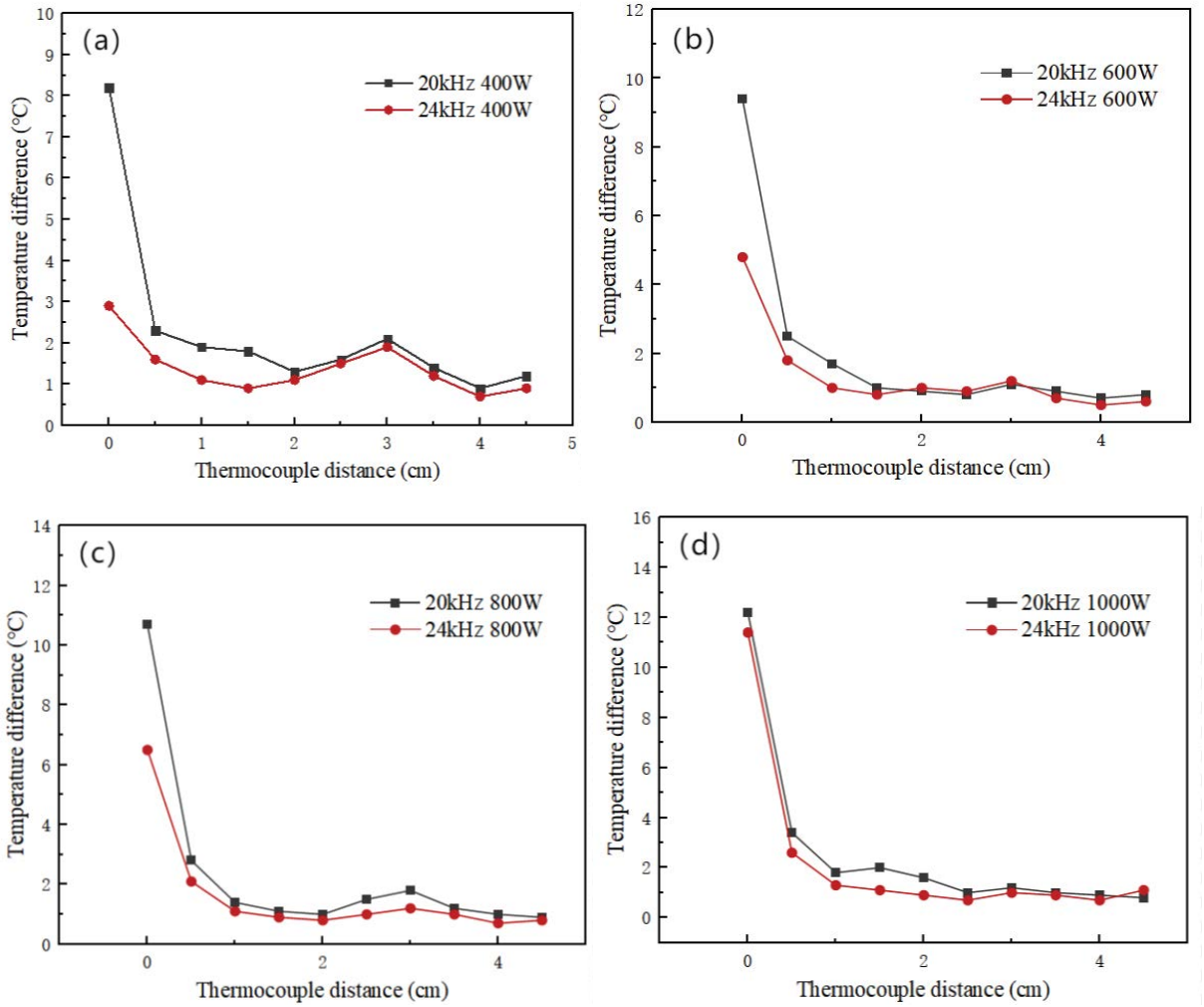

Fig. 7. Variation curves of sound field intensity along the axial direction of the probe at (a) 20 kHz, 24 kHz, 400 W, (b) 20 kHz, 24 kHz, 600 W, (c) 20 kHz, 24 kHz, 800 W and (d) 20 kHz, 24 kHz, 400 W.

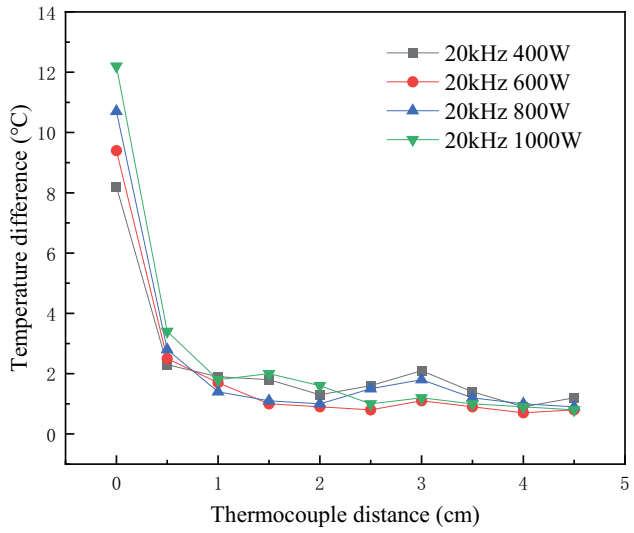

Fig. 8. Curves of cavitation intensity vs. ultrasonic power at 20 kHz at various distances.

length is due to the reflection of the ultrasonic waves at the cup wall, forming a standing wave, thus increasing the local sound intensity near the probe.

3.3.3. Change ultrasonic power

By keeping other parameters constant and using the optimized ultrasonic frequency at 20 kHz, the axial variation law of the cavitation effect is investigated by changing ultrasonic power, and its influence on ultrasonic cavitation is also studied. The experimental results are shown in Fig. 9.

As seen in Fig. 9, when the ultrasonic frequency is kept at 20 kHz, there is a positive correlation between the power and the cavitation effect, and the sound intensity gradually increases with the increase of ultrasonic power, which is consistent with the numerical simulation results of ultrasonic cavitation bubbles. Therefore, a better understanding of the relationship between the cavitation effect and each influencing factor will assist in designing and developing a potential ultrasonic sludge sonochemical reactor.

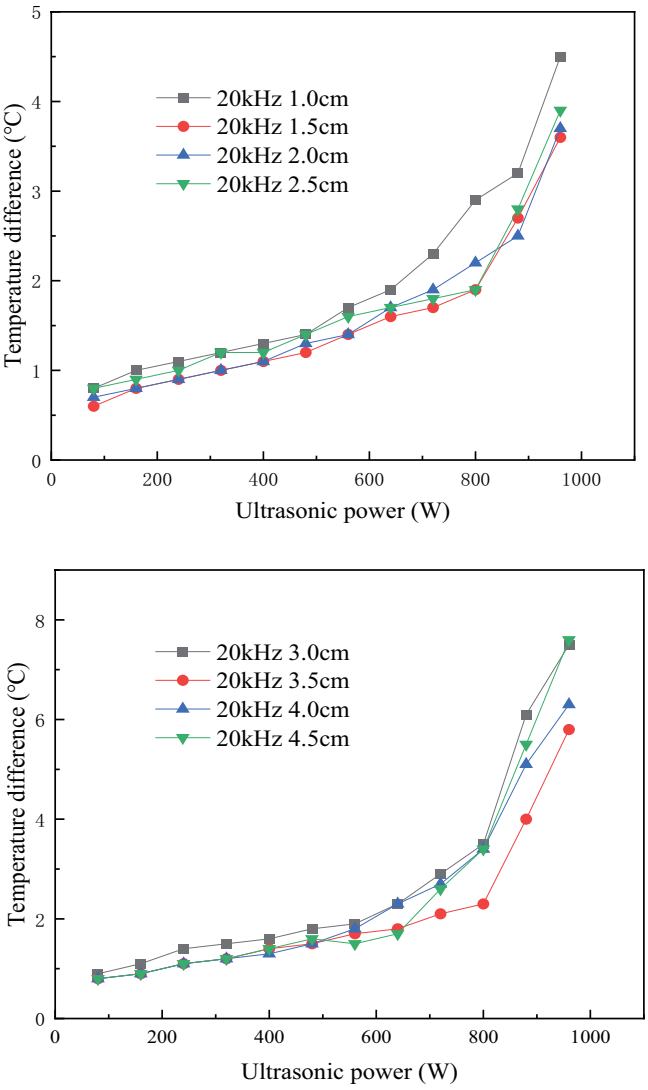

Fig. 9. Curves of cavitation intensity along the axial direction of the probe at 20 kHz at various power intensities.

3.4. Ultrasonic experimental analysis

Combined with the above analysis, the best effect was identified when the ultrasonic frequency was 20 kHz. In this part, the microscopic changes of sludge, SCOD content, protein content, polysaccharide value, and total suspended solids (TSS) content in the supernatant after ultrasonic treatment of excess sludge are assessed to analyze the effect of ultrasonic treatment on sludge cracking.

3.4.1. Sludge morphology analysis

Scanning electron microscopy (SEM) images before and after ultrasonic cracking of excess sludge are shown in Fig. 10. Fig. 10a shows an SEM image of excess sludge before ultrasonic treatment and Fig. 10b of excess sludge after ultrasonic treatment with ultrasonic power of 1,000 W for 15 min. Before treatment, the surface of the original excess sludge appears compact and smooth, exhibiting good integrity and forming layered structures. However, after ultrasonic treatment, the surface structure of excess sludge appears rough, loses its integrity, and transforms into a layered-block structure stacked together. The appearance of this structure is mainly attributable to the microbial micelles and microbial cell wall structure in sludge being destroyed, dispersed, and stacked into many flocculent structures. This leads to reduced microbial activity that is beneficial to stabilizing and reducing sludge.

3.4.2. Analysis of sludge particle size

The frequency distribution curves of the particle size of the sludge samples before and after ultrasonic treatment are shown in Fig. 11. As can be seen from Fig. 11a, the particle size of the original sludge was mainly distributed between 10 and 100 μm, d_{50} = 34.82 μm as measured by the laser particle sizer. After ultrasonic treatment at 20 kHz with 1,000 W and a treatment time of 30 min, as can be seen from Fig. 11b, the particle size of the sludge was mainly in the range of 1–10 μm, with d_{50} = 2.99 μm, and some of the sludge particles smaller than 1 μm, reaching the nanometer scale.

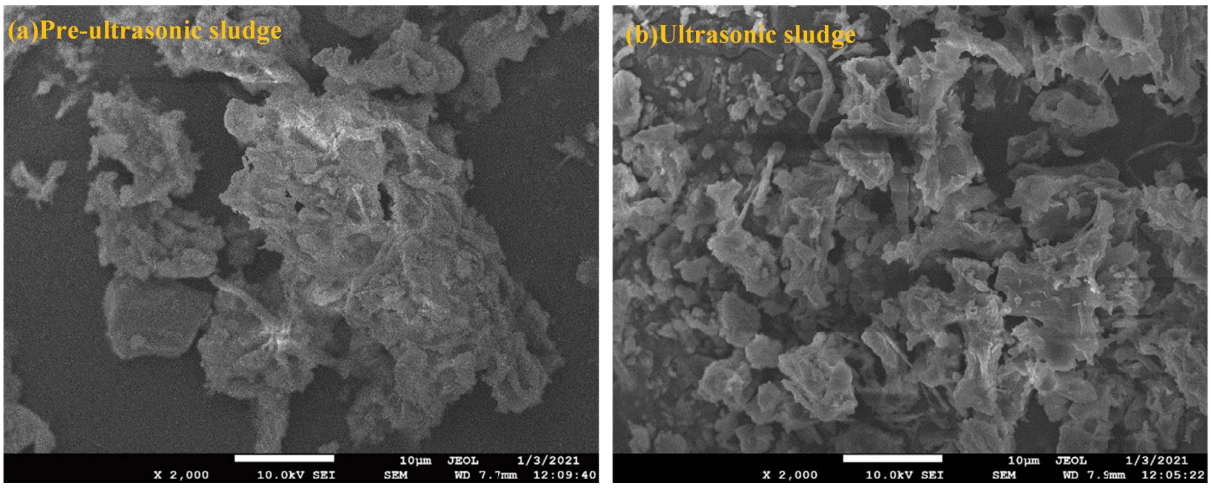

Fig. 10. Scanning electron microscopy images of the morphology of (a) original sludge and (b) ultrasonic sludge.

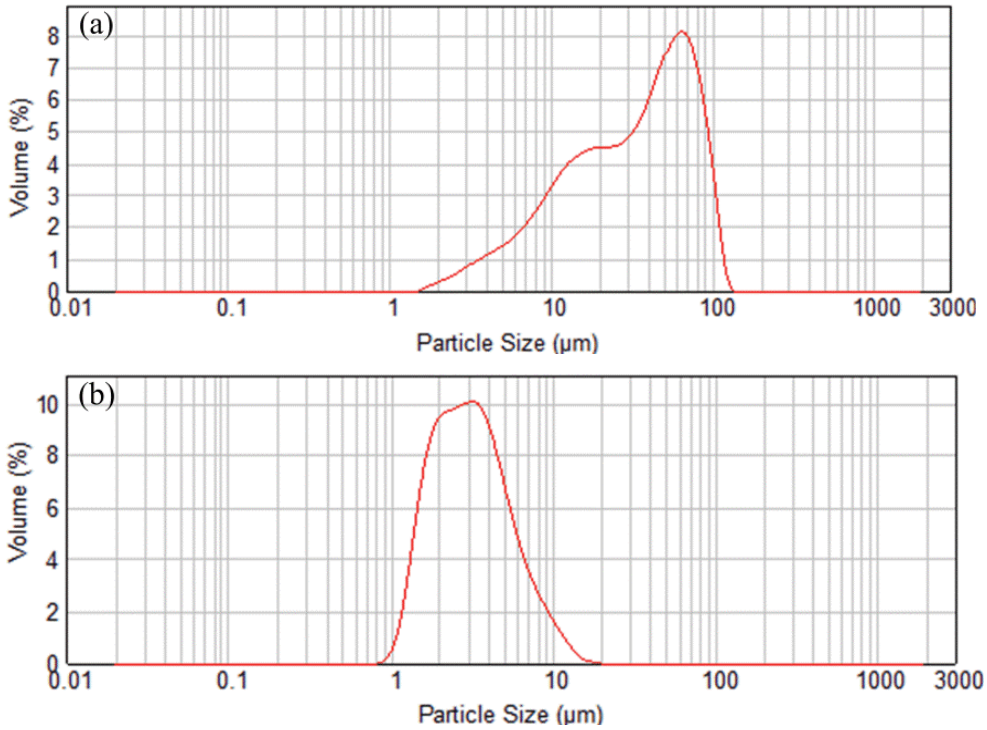

Fig. 11. Particle–size distribution curves of (a) original sludge and (b) ultrasonic sludge.

These nanoparticles adsorb onto microbial cells, rendering them inactive and creating a concentration gradient that spreads, resulting in a more stable sludge.

The results show that, after ultrasonic treatment, the mycolloids in the excess sludge were broken up by ultrasonic treatment and lost their original water-locking properties, resulting in increased dewatering of the excess sludge and making it more stable, thus achieving sludge reduction.

3.4.3. Biochemical analysis

The excess sludge contains a large number of microorganisms, bacteria, and other organic substances. Ultrasonic cracking will cause the microbial cells in the excess sludge to crack, resulting in the outflow of organic substances from the cytoplasm. Thus, the effect of ultrasonic cracking on the excess sludge can be characterized by the SCOD value, protein content, polysaccharide content, and TSS reduction rate in the supernatant. Fig. 12 shows the value variation in SCOD, protein content, polysaccharide content, and TSS reduction rate over time in different conditions of ultrasonic powers. As shown in Fig. 12, all values increase with increased time and ultrasonic power.

When the ultrasonic power is 270 W, the curves change slowly over time. After 30 min of sonication, the SCOD increased from 96 to 522 mg/L, the protein dissolution increased from 33.20 to 98.43 mg/L, the polysaccharide dissolution increased from 6.89 to 53.83 mg/L, and the TSS reduction rate increased from 8.7% to 34.9%, indicating that the ultrasonic cannot effectively destroy the cell structure in the excess sludge under this condition.

When the ultrasonic power is 450 and 630 W, the growth trend of each curve is roughly the same, and the difference in index content is not significant; however, the result is marginally better at 630 W than it is at 450 W. After 30 min of sonication, the SCOD increased from 96 to 2,285 and 2,660 mg/L, the protein dissolution from 64.07 and 83.60 mg/L to 145.13 and 150.73 mg/L, the polysaccharide dissolution from 19.52 and 38.08 mg/L to 84.26 and 115.98 mg/L, and the TSS reduction from 10.7% and 12.1% to 35.4% and 48%.

When the ultrasonic power is 900 W, both the index content and growth rate are clearly enhanced. After 30 min of sonication, the SCOD increased from 96 to 4,070 mg/L, the protein dissolution increased from 112.26 to 258.52 mg/L, the polysaccharide dissolution increased from 49.95 to 186.87 mg/L, and the TSS reduction rate increased from 13.6% to 54.2%. It is mainly because the cell wall, cytoplasm, and cell membrane of microorganisms in the sludge are broken by ultrasonic waves at high power for a long time, leading to a larger increase in the content of each index. From the above index analysis, it is clear that ultrasonic cracking of excess sludge does have a good effect.

3.5. Ultrasonic sludge resource utilization analysis

Based on changes in the levels of indicators in the sludge supernatant, ultrasonic treatment of sludge can be divided into three stages: floc disruption, cell wall disruption, and cytoplasmic efflux. The release of organic matter from the sludge by ultrasonic can benefit subsequent research on sludge resources. For example, the organic matter concentrate released from the sludge can be used as organic fertilizer for green plants, and the protein concentration of the

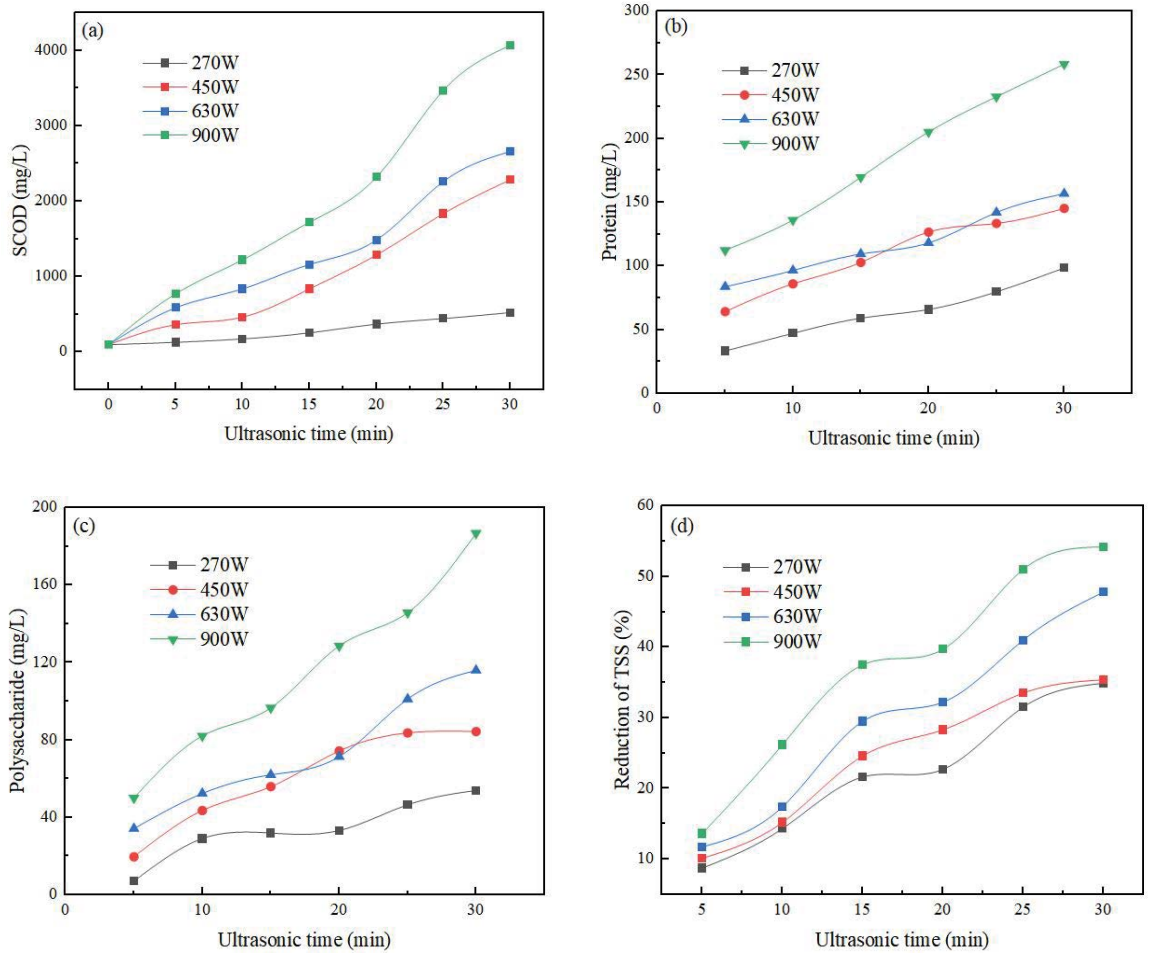

Fig. 12. Content of (a) SCOD, (b) protein, (c) polysaccharide, and (d) total suspended solids in the supernatant of the excess sludge after ultrasonic treatment.

supernatant can be processed into protein products such as protein foam fire extinguishers. In addition, the particle size of the remaining sludge is significantly smaller after ultrasonication, and the colloids and microorganisms are broken down by ultrasonication, greatly reducing the water retention and biological activity of the sludge and increasing its stability, which is beneficial for the subsequent resource utilization of the sludge in the agricultural and construction industries.

4. Conclusion

According to the numerical simulation results, it can be seen that a better ultrasonic cavitation effect can be obtained by using a lower ultrasonic frequency and larger ultrasonic power. Moreover, the cavitation experimental results are consistent with the numerical simulation. Through microscopic particle size and biochemical analysis, it can be seen that ultrasonic waves do have a better effect on sludge fragmentation, the microbial micelle and cell wall structure in the sludge are destroyed, and sludge dewatering and stability are improved. Therefore, numerical simulations can be integrated with experiments to understand the ultrasonic wave propagation law in excess sludge and to realize the resourcefulness and stabilization of the excess sludge.

Declaration of competing interest

The authors declare that they have no known competing financial interests or personal relationships that could have appeared to influence the work reported in this paper.

Acknowledgment

This work was supported by the Key R&D Program Project of the Ministry of Science and Technology: Research and Demonstration of Near-Zero Discharge and Resource Utilization Technology of Industrial Wastewater in High-tech Zone (No.2019YFC0408500).

References

[1] Z. Runjie, G. Chunyu, Z. Shiwen, Q. Yue, T. Lili, F. Baorong, Response mechanism of water ecosystem under the influence of urbanization: a case study of the connection zone between Shenyang and Fushun, Meteorol. Environ. Res., 9 (2018) 15–18.

[2] N. Mehrdadi, F.G. Kootenaei, An investigation on effect of ultrasound waves on sludge treatment, Energy Procedia, 153 (2018) 325–329.
[3] H. Guo, Y. Wang, L. Tian, W. Wei, T. Zhu, Y. Liu, Unveiling the mechanisms of a novel polyoxometalates (POMs)-based pretreatment technology for enhancing methane production from waste activated sludge, Bioresour. Technol., 342 (2021) 125934, doi: 10.1016/j.biortech.2021.125934.
[4] J. Zhang, D. Xu, G. Zhang, Z. Ren, Y. Zhu, Critical review on ultrasound lysis-cryptic growth for sludge reduction, J. Environ. Chem. Eng., 9 (2021) 106263, doi: 10.1016/j.jece.2021.106263.
[5] P.E.E. Maye, Y. Jingyi, Y. Taoyan, X. Xinru, Study on the modification of vacuum residue by ultrasonic radiation, China Pet. Process. Petrochemical Technol., 19 (2017) 114–122.
[6] X. Zhang, X. Zheng, P. Han, Z. Liu, L. Chang, Effects of ultrasound on the desulfurization performance of hot coal gas over Zn-Mn-Cu supported on semi-coke sorbent prepared by high-pressure impregnation method, J. Energy Chem., 24 (2015) 291–298.
[7] Ł. Skórkowski, E. Zielewicz, A. Kawczyński, B. Gil, Assessment of excess sludge ultrasonic, mechanical and hybrid pretreatment in relation to the energy parameters, Water, 10 (2018) 551, doi: 10.3390/w10050551.
[8] A.P. Bhat, P.R. Gogate, Cavitation-based pre-treatment of wastewater and waste sludge for improvement in the performance of biological processes: a review, J. Environ. Chem. Eng., 9 (2021) 104743, doi: 10.1016/j.jece.2020.104743.
[9] D. Yuan, X. Zhou, W. Jin, W. Han, H. Chi, W. Ding, Y. Huang, Z. He, S. Gao, Q. Wang, Effects of the combined utilization of ultrasonic/hydrogen peroxide on excess sludge destruction, Water, 13 (2021) 266, doi: 10.3390/w13030266.
[10] A. Xu, G. Zhang, Y. Ying, C. Wang, Complex fields in heterogeneous materials under shock: modeling, simulation and analysis, Sci. China Phys., Mech. Astron., 59 (2016) 1–49.
[11] M. Ahmadi Khoshooei, Thermal probe of vapor–liquid thermodynamic equilibrium, J. Therm. Anal. Calorim., 147 (2022) 6015–6034.
[12] M.S. Plesset, R.B. Chapman, Collapse of an initially spherical vapour cavity in the neighbourhood of a solid boundary, J. Fluid Mech., 47 (1971) 283–290.
[13] Y. Sun, J. Xiang, M. Liang, S. Huang, Y. Mao, Research on the influence factors of ultrasonic cavitation on particle breakage, J. Zhejiang Univ. Technol., 47 (2019) 146–150+157.
[14] R. D'Ambrosio, C. Scalone, Two-step Runge–Kutta methods for stochastic differential equations, Appl. Math. Comput., 403 (2021) 125930, doi: 10.1016/j.amc.2020.125930.
[15] K.A. Koroche, Numerical solution of first order ordinary differential equation by using Runge–Kutta method, Int. J. Syst. Sci. Appl. Math., 6 (2021) 1–8.
[16] P. Cao, C. Hao, C. Ma, H. Yang, R. Sun, Physical field simulation of the ultrasonic radiation method: an investigation of the vessel, probe position and power, Ultrason. Sonochem., 76 (2021) 105626, doi: 10.1016/j.ultsonch.2021.105626.
[17] S.W. Fong, E. Klaseboer, C.K. Turangan, B.C. Khoo, K.C. Hung, Numerical analysis of a gas bubble near bio-materials in an ultrasound field, Ultrasound Med. Biol., 32 (2006) 925–942.
[18] M. Mendonck, S. Aparicio, C. González Díaz, M.G. Hernández, G.M. Muñoz Caro, J.J. Anaya, S. Cazaux, Ultrasonic propagation in liquid and ice water drops. effect of porosity, Sensors, 21 (2021) 4790, doi: 10.3390/s21144790.
[19] L. Xuefeng, The Study of Sound Field Characteristics and its Corresponding Distribution Regularities in Continuous-Flow Ultrasonic Reactors, South China University of Technology, 2015.
[20] Y. Asakura, K. Yasuda, Frequency and power dependence of ultrasonic degassing, Ultrason. Sonochem., 82 (2022) 105890, doi: doi: 10.1016/j.ultsonch.2021.105890.
[21] G.S.B. Lebon, I. Tzanakis, G. Djambazov, K. Pericleous, D.G. Eskin, Numerical modelling of ultrasonic waves in a bubbly Newtonian liquid using a high-order acoustic cavitation model, Ultrason. Sonochem., 37 (2017) 660–668.
[22] J. Liang, X. Wu, Y. Qiao, Dynamics of twin bubbles formed by ultrasonic cavitation in a liquid, Ultrason. Sonochem., 80 (2021) 105837, doi: 10.1016/j.ultsonch.2021.105837.
[23] L. Ye, X. Zhu, Y. Liu, Numerical study on dual-frequency ultrasonic enhancing cavitation effect based on bubble dynamic evolution, Ultrason. Sonochem., 59 (2019) 104744, doi: 10.1016/j.ultsonch.2019.104744.
[24] X. Guo, Y. Yang, X. Li, Z. Zhou, S. Ji, X. Han, S. Wang, Q. Zeng, H. Zhan, Measurement and visualization of ultrasonic cavitation field based on MATLAB, China Environ. Sci., 36 (2016) 719–726.
[25] M. Wang, D. Zheng, J. Dong, Y. Xu, Comparison of ultrasonic attenuation models for small droplets measurement based on numerical simulation and experiment, Appl. Acoust., 183 (2021) 108334, doi: 10.1016/j.apacoust.2021.108334.
[26] H. Dong, X. Yang, J. Tang, Y. Lü, G. Yue, Ultrasound intensity distribution measurement using a thermoelectric probe, J. Harbin Eng. Univ., 33 (2012) 911–915.